Proper Orthogonal Decomposition used for determination of the convection velocity of the initial zone of the annular jet. Aerodynamic study and control of instabilities

Béatrice Patte-Rouland, Amélie Danlos, Gildas Lalizel, Eric Rouland, Pierre Paranthoen

Proper Orthogonal Decomposition used for determination of the convection velocity of the initial zone of the annular jet. Aerodynamic study and control of instabilities.

B.PATTE-ROULAND, A.DANLOS, G.LALIZEL, E.ROULAND*, P.PARANTHOEN.

Laboratory of Thermodynamic CORIA UMR 6614, Rouen University
* AREELIS Technologies
Avenue de l'université BP 12 76230 Saint -Etienne du Rouvray
FRANCE
beatrice.patte@coria.fr http://www.coria.com

Abstract: - The annular jet is an example of complex shear flow situations. Two axisymmetric shear layers, originating at the jet exit, one at the nozzle lip and the other at the centre body, eventually meet downstream or interact with each other. This study also proposes to apply P.O.D on P.I.V velocity fields. We propose especially a determination of the convection velocity of the primary vortices of an annular jet. In this study, we want to investigate two ways to reduce the stagnation point instabilities of an annular jet with a large diameter ratio (r=0.91). This article discusses the application of Proper Orthogonal Decomposition to the P.I.V. velocity fields of an annular jet and on a statistic of time-resolved tomographic images of the initial zone of the annular jet. In the second part of the study, the influence of the internal obstacle shape is studied. We will also use P.I.V. measurements to see the effects of three internal obstacles: a disk, a cone and a spheroid. The main aim of this study is to observe and analyze the effects of different annular jet configurations, in order to find a new way to reduce jet instabilities, using passive or active control. The second method consists in applying a sound wave to obtain an active control of these instabilities. With different frequencies (fundamental, first harmonic…), we will see the effect on the flow by the P.I.V. measurement technique (Particle Image Velocimetry). Measurements are conducted with a Reynolds number Re_{Do}=107800. The fluctuation frequency of the stagnation point is known for this Reynolds number. The Strouhal number corresponding to this frequency is St_{Do} = 0.27. Active control has already been used with round jets and has given promising results, but only a few studies have been conducted on annular jets in this field. This work will permit us essentially to have a better knowledge of annular jets and to meet manufacturers' needs.

Key-Words: - Particle Image Velocimetry, Proper Orthogonal Decomposition, Annular jet, Convection velocity, control, acoustics excitations.

1 Introduction

Annular jet is used in the industrial domain, in combustion (burners, bluff bodies…) or in industrial treatment processes. The geometry of the annular jet is determined by the ratio D_i/D_o, where D_i represents the internal diameter and Do the external diameter. The flow characteristics of the initial region of an annular jet discharging into stationary air have been investigated previously. Chigier [1], in 1964, studied them as a limiting case of coaxial jets. Because the configuration of the annular jet often adopted by authors was without after body or bullet at the nozzle exit, an internal recirculating region is formed downstream of the interface. This recirculation zone is the result of the lack of any air supply in the center and the entrainment of air from the main stream of the annular jet. The interests of the flow here are the interaction between the jet and the recirculation zone near the nozzle of the annular jet. Many authors, like Ko [2][3], work on small diameter ratio annular jets, with a ratio D_i/D_o smaller than 0.7. Only the fully-developed merging zone of a diameter ratio larger than 0.7 have been studied by Aly [4] in 1991.

The scientific interest in the study of turbulence has led to the development of a P.I.V. post-processing, which is able to bring out the inner driving mechanism of the flow [5]. In other words, the structure responsible for the development or the maintenance of flow instability has to be reached. So, in this context, Lumley [6] [7] has proposed a method for identifying coherent and instantaneous structures in turbulent flow. The method is the Proper Orthogonal Decomposition (P.O.D.). This method provides a base for the modal decomposition of a set of functions, such as data obtained in the course of the experiments. The most striking property of this decomposition is optimality: it provides the most efficient way of capturing the dominant components of an infinite-dimensional process with only a few functions. That is why the P.O.D. process has been applied in different turbulent flows to analyze

experimental P.I.V. data with a view to extracting dominant features and trends : coherent structures [6][7][8][9]. P.O.D. provides an optimal set of basis functions for an ensemble of data. It is optimal in the sense that it is the most efficient way of extracting the most energetic component of an infinite dimensional process with only a few modes [5]. The present study relies on an experimental investigation of the initial zone of a large diameter ratio annular air jet by the use of Particle Image Velocimetry (P.I.V.), fast tomography imagery. The intention of the present investigation is to dissociate the oscillation and velocity fluctuations due to the turbulent flow behavior. So it is useful to establish the link between the first P.O.D. eigenfunctions and the motion of the stagnation point at the end of the annular jet recirculation zone. Then, measurements of convection velocity will be determined by the use of a Proper Orthogonal Decomposition (P.O.D.) mode applied on tomographic images of an annular jet. In a second part, the present study relates to the study of the influence of the geometry of the internal obstacle (conical, spheroidal and disc) on the morphology of the jet. The other part presents the influence of acoustic waves on instabilities of stagnation point of an annular jet.

2 Experimental set-up

2.1 Annular jet

A diagram of annular jet is shown in fig 1. The annular jet is characterized by the outer diameter Do, equal to 53.88 mm, and the inner diameter D_i, equal to 48.75 mm. The thickness of the jet e is thus equal to 2.565 mm. In our setup, D_i/D_o is equal to 0.90. The exit velocities U_o are equal to 8 m/s, 15 and 30m/s which respectively correspond to the values of the Reynolds number Re, based on the thickness e, of 2048, 3840 and 7680. At a distance from the nozzle of 50 μm, the cross sectional profile of the longitudinal, measured with hot wire anemometry, shows a "top hat" distribution.

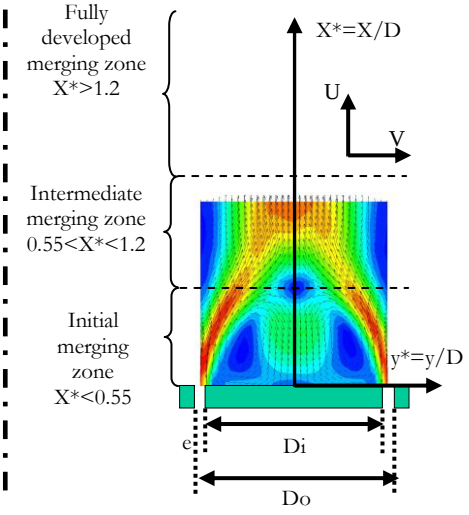

Fig 1: annular jet

2.2 Cross correlation PIV set-up

The experimental setup of the P.I.V. measurements is presented in fig 2. A double pulsed Nd-Yag laser is used to set up the light sheet. The output energy is nearly 30 mJ for each laser pulse. The wavelength is 532 nm. The laser beams are focused onto a sheet across the median plane of the annular jet by one cylindrical lens (f=-0.02 m) and one spherical lens (f=0.5 m). The time delay between the two pulses, which depends on the exit velocity U_o, is 8 μs. The observation field is 2.8*2.5 cm².

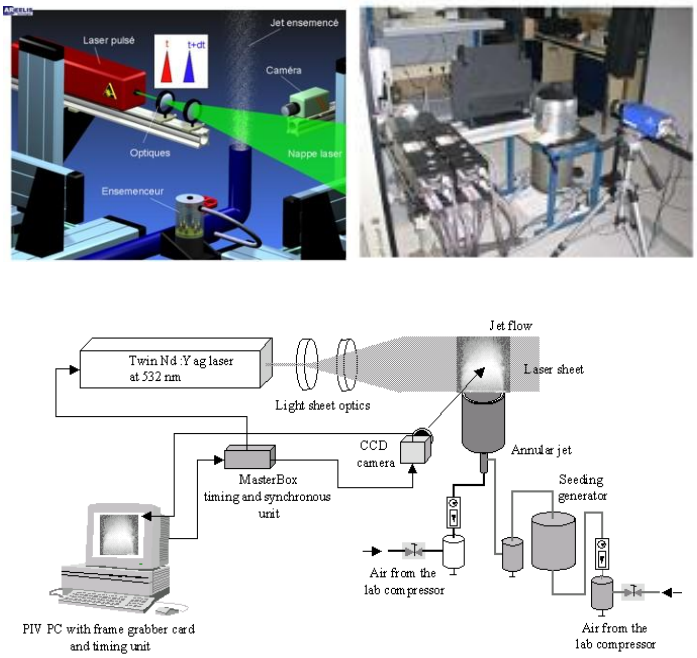

Fig 2: experimental PIV set-up

In this study, the video images are recorded by a LAVISION Flow Master 3S camera. The frame grabber, using a pixel clock, digitizes the analogue video signal to an accuracy of 12 bits. In the frame grabber, each field is digitized in 1280*1024 pixels with grey levels. The acquisition frequency is 4 Hz. Interrogation of the recorded images is performed by two-dimensional digital cross correlation analysis using "Davis 6.2.2." For all velocity fields, the sampling window has a size of 16 by 16 pixels (0.377 by 0.377 mm) and there is a 50 % overlap with the next window. 400 P.I.V. images have been recorded. We observed less than 1 % of false vectors calculated in the flow.

2.3 Acoustics

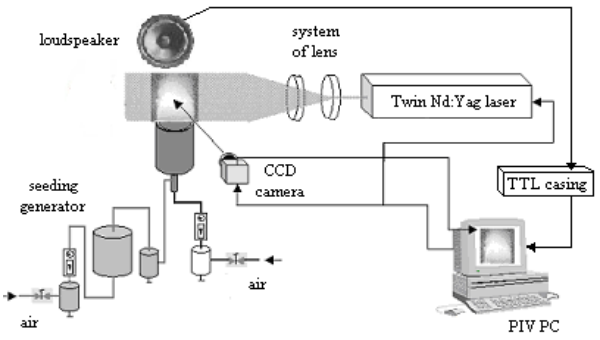

Fig 3: experimental set-up for the study of active control

The majority of works concerning the active control of the annular jets are carried out with measurements by hot wire anemometry or visualizations. Nakazano and Al [10], in 1991 work on basic annular jets of diameter ratio ranging between 0.2 and 0.8. They discover that for a frequency of excitation equal to the frequency of formation of the swirls, the recirculation zone can be influenced and the length of this one can even decrease. Travnicek and Tesar [11] work on an annular impinging jet of diameter ratio 0.95 and notice that they can, in the absence of wall, influence the initial zone by using acoustic excitations of frequencies corresponding to frequencies of formation of the swirls. They note that the harmonic and double excitation harmonic cause the increase or the suppression of the appearance of the swirls. The Strouhal numbers for this study are between 0.38 and 2.47.

2.4 Fast tomographic imaging set-up

The laser sheet is obtained by a 4W, 515nm Argon-Ion continuous laser. The tomography system is composed of a high-speed digital camera Kodak Ektapro 8 bits. For the annular jet we used 256x256 pixels at 4500 images/s. For the round jet, we used 128x256 pixels, 0.13mm/pixels at 9000 images/s.

2.5 Flow seeding.

Flow seeding is one of the most important aspects of P.I.V. measurements. The intake air is seeded with 2-3 µm diameter olive oil droplets. These were generated in an atomizer by passing air through a bath of olive oil. The air pressure varied from 1.5 to 2.5 bars (fig 2). The particle seeding density was controlled by the flow rate of air through the atomizer.

3 Proper Orthogonal Decomposition.

Coherent structures are present in turbulent flow and P.I.V. is able to highlight those on the largest scale at any given moment. The scientific interest in the study of turbulence has led to the development of P.I.V. post-processing, which is able to bring out the inner driving mechanism of the flow [5].

Lumley [6] [7] has proposed a method for identifying coherent and instantaneous structures in turbulent flow. The method is Proper Orthogonal Decomposition (P.O.D.). P.O.D. provides an optimal set of basis functions for a set of data, Delville [12], Graftieux [13], Sirovish [13], Patte-Rouland [14]. It is optimal in the sense that it is the most efficient way of extracting the most energetic components of an infinite dimensional process with only a few modes. The proper orthogonal decomposition is a linear procedure, which decomposes a set of signals in modal base. The P.O.D. analysis is introduced in this context by the use of physical functions with finite kinetic energy equivalent to the square integrable function. Coherent structures should be the structures that have the largest mean square projection on the velocity field. If it represents the candidate structure, then:

$$\frac{\left\langle (U.\Phi)^2 \right\rangle}{\left\langle (U.U)^2 \right\rangle} = \max_{\Psi} \frac{\left\langle (U.\Psi)^2 \right\rangle}{\left\langle (U.U)^2 \right\rangle} \qquad (1)$$

Where $\langle\ \rangle$ represents an ensemble average. That is, the field that maximises the inner product with the velocity field is found. Maximising this inner product leads to the solution of the following eigenvalue problem:

$$\iint_D \left\langle U(x)U^*(x') \right\rangle \Phi(x')dx' = \lambda.\Phi(x) \qquad (2)$$

Or in another way,

$$\iint_D R_{ij}(x,x').\Phi_j^{(n)}(x')dx' = \lambda^{(n)}\Phi_i^{(n)}(x) \qquad (3)$$

D represents the two dimensional domain of the velocity fields. R is the averaged two-point correlation tensor defined by:

$$R_{ij}(x,x') = \left\langle U_i(x).U_j(x') \right\rangle \qquad (4)$$

The solutions of (3) represent a set Φ_k of base functions where each velocity field Ui is:

$$U_i = \sum_{k=0}^{N-1} a_{k,i}\Phi_k \qquad (5)$$

Then the eigenfunctions Φ can be of the following form:

$$\Phi = \sum_{k=0}^{M-1} A_k U^{(k)} \qquad (6)$$

We will order the eigenvalue by λ_i $i>\lambda_{i+1}$ and since R is non negative we can be sure that $\lambda_i > 0$ ($\forall$ i $\in$ N).

Each velocity fields can be decomposed as a linear combination of proper mode ϕ such that:

$$u_i(x,y)=\sum_{k=0}^{N-1} a_{i,k}\phi_k(x,y) \text{ and } \delta_{kk'}\lambda_k=\left\langle a_k a_{k'}^{*}\right\rangle \qquad (7)$$

Where λ_k is the energy contained in the mode k. The computation has been done with 400 velocity fields. This number is sufficient for a good representation of the flow.

4. Velocity characteristics of annular jet.

4.1 Aerodynamic characteristics of the initial zone of annular jet.

For the annular jet, it appears that the stagnation point is put through important radial fluctuations and, axially, the maximal fluctuations are localized on the external-mixing layer. This was also observed by Ko and Chan [3], but they used a hot wire and this cannot measure null velocity. Therefore, for a spatial quantification, the P.I.V. technique has been used [9].

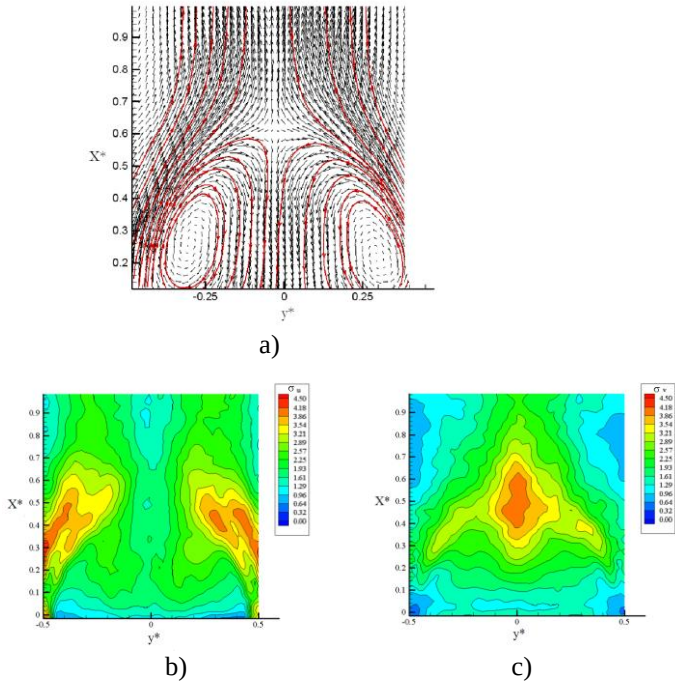

Fig 4: Aerodynamic characteristics of the annular jet: Re_e = 7680. a) Average velocity field calculated with 400 P.I.V. fields. b) Reynolds decomposition radial velocities c) Reynolds decomposition axial velocities.

Figure 4 shows an example of the mean velocity field with the corresponding Reynolds decomposition fluctuation fields. The initial merging zone extends from the jet exit to the tip of the potential core. This zone contains a recirculating zone. The stagnation point which marks the end of the recirculating region is located at x/Do=0.5.

4.2 Results of Proper Orthogonal Decomposition application

In this study the P.O.D. is applied on P.I.V. velocity fields of the recirculation zone of this annular jet. Reynolds decomposition velocity fluctuations show two effects: the importance of oscillations for the stagnation point and the air entrainment in the annular jet. Thus, to evaluate the importance and the influence of each mode on an instantaneous velocity field, each instantaneous field reconstructed by choosing P.O.D. modes, and then the Reynolds decomposition radial fluctuations are calculated. A reconstruction with the first mode and the k^{th} mode, using the projection value of the instantaneous field on the modes, automatically shows what instability is represented by this k^{th} mode. Fig 5 shows the reconstruction of all the instantaneous fields with the first two modes and without mode 1. So, it is clear that with modes 0+1 the position and the intensity of the Reynolds decomposition radial fluctuations are the same as those calculated for all modes, contrary to the reconstruction without mode 1. So mode 1 is responsible for the radial fluctuations of the stagnation point.

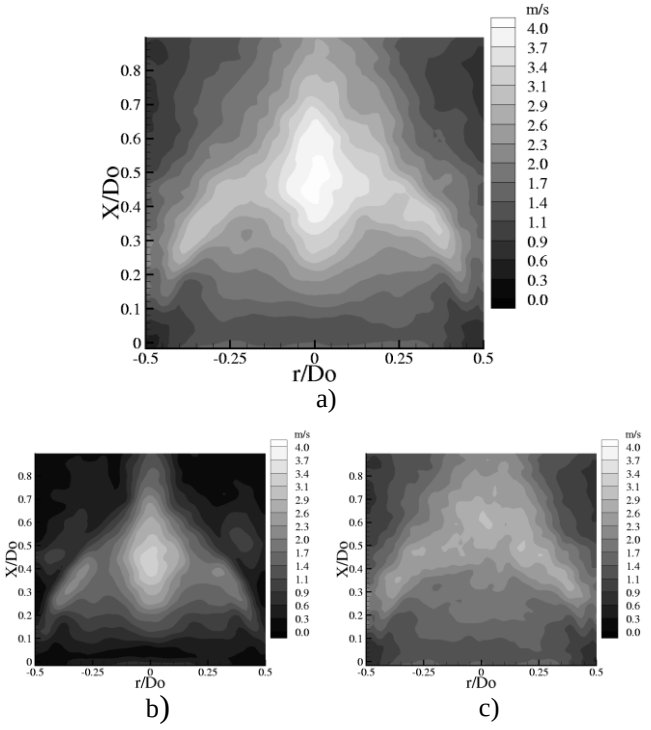

Fig 5: Influence of mode 1 on Reynolds decomposition radial velocity fluctuations: a) Radial velocity fluctuations b) Radial

velocity fluctuations reconstructed with mode 0 and 1. c) Radial velocity fluctuations reconstructed without mode 1.

5 Determination of the convection velocity U_c.

Two different methods have been applied to determine the convection velocity U_c of the primary vortices.

5.1 Velocity convection of the primary vortices of the annular jet determined by classical method.

The first one consists in determining U_c by calculating the ratio between a distance d and a time. The distance is measured between two primary vortices, and the time is determined from the frequency of appearance f of the vortices.

An algorithm for the detection of the core of a vortex has been used to measure the probability density function of the distance between two primary vortices. The algorithm was developed by Graftieux [11]. S is the area of a mesh, centered on a point P. U_M is the velocity at a point M included in S. Γ is thus a scalar function and its value lies between –1 and +1, according to the direction of rotation of the axisymmetric vortices.

$$\Gamma(P)=\frac{1}{S}\int_S \frac{\overrightarrow{PM}\wedge\overrightarrow{U_M}}{\left\|\overrightarrow{PM}\right\|\wedge\left\|\overrightarrow{U_M}\right\|}dS \qquad (8)$$

This algorithm has been applied to all the velocity fields for all U_o velocities. Thus, we have calculated the PDF of inter-vortex distances d in the external (Fig 6) and internal (Fig 7) mixing layers. There are significant real differences between the two layers.

In the external layer, the more probable distance d_m is about 0.06. There is also, for U_o =8 m/s, a second peak localized for d/D_o=0.12. This represents the distance between paired vortices, double of the distance d_m.

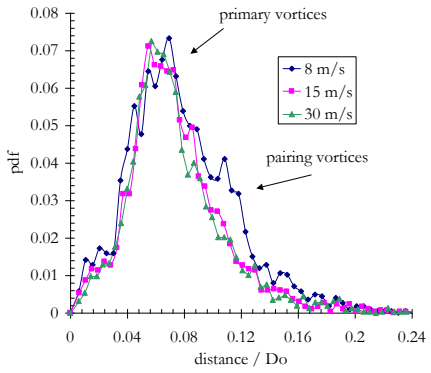

Fig 6: Probability density function of the distance d_m for U_o=8, 15 and 30 m/s. External layer of annular jet.

In the internal mixing layer, the distance d_m depends on the velocity U_o. At the beginning of the internal shear layer, a small recirculation zone defined in the previous part influences the convection velocity of the vortices. The frequency, measured by hot wire anemometry, is the same as the frequency of the external mixing layer. Because the distance d_m is different according to the velocity, U_c* is not a constant.

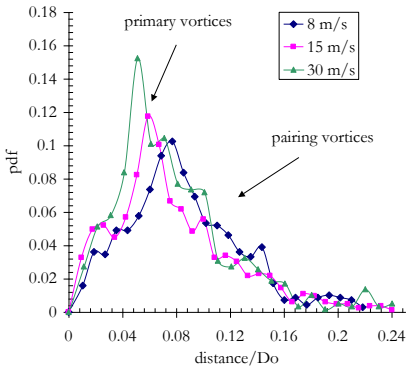

Fig 7: Probability density function of the distance d_m for U_o= 8, 15 and 30 m/s. Internal mixing layer of annular jet.

The results of the determination of the convection velocity U_c * of primary vortices are:

	external mixing layer			internal mixing layer		
Uo (m/s)	8	15	30	8	15	30
Uc*	**0.31±0.03**	**0.27±0.02**	**0.28 ± 0.02**	**0.39±0.03**	**0.27±0.02**	**0.24±0.02**

Table 1: determination of the convection velocity

5.1.2 Velocity convection of the primary vortices of the annular jet determined by classical P.O.D.

The second method is an application of an inhomogeneous filter called Proper Orthogonal Decomposition (P.O.D.) on a statistic of time-resolved tomographic images of the initial zone of the annular jet. It can be applied on scalar fields, such as images (Sirovich [12] [13]), or P.I.V. fields (Patte-Rouland [14]). P.O.D. is optimal in the sense that it is the most efficient way of extracting the most energetic component of an infinite dimensional process with only a few modes. As relation (1), each image can be decomposed as a linear combination of proper mode ϕ such that:

$$\mathrm{Im}_i(x,y)=\sum_{k=0}^{N-1} a_{i,k}\phi_k(x,y) \qquad (9)$$

The computation has been done with 400 images for U_o=8 m/s. The first five different modes are displayed on the figure 8. The first one has the topology of the mean image of the flow. The other modes are characteristic of a convection flow. Each presents an alternation of positive and negative zones in the external mixing layer. The

negative values of a mode are represented by a black pixel and positive values by a white one.

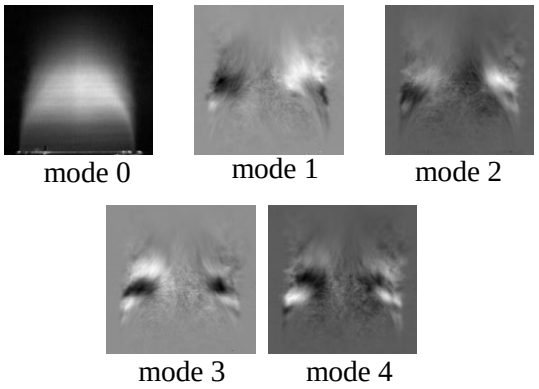

Fig 8: The first 5 modes calculated from P.O.D., for U_o=8 m/s.

The mode 3 and mode 4 show an alternation of black and white zones in the external mixing layer of the annular jet. The temporal evolution of a_3 and a_4 shows a frequency equal to 249 Hz for the two modes. We can determine a characteristic distance d_p, as the length of a white, or black zone.
In figure 9a, is plotted the evolution of the reconstruction coefficient of modes 3 and 4.

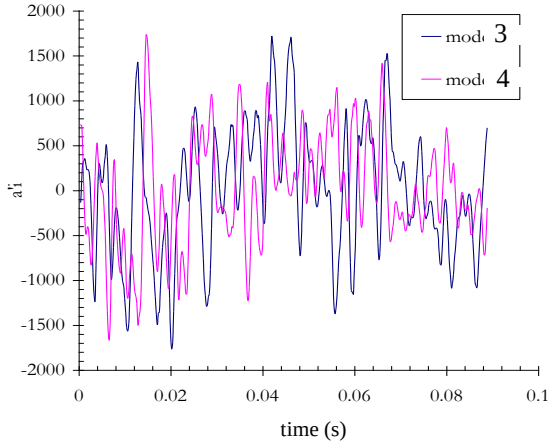

a)

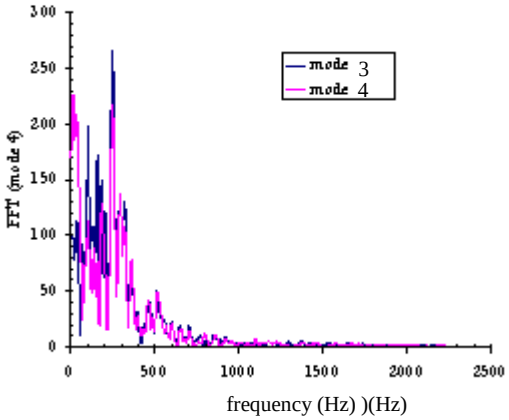

b)

Fig 9: a) Temporal evolution of the reconstruction coefficient of the mode 4 and 5, b) FFT of a).

By applying a Direct Fourier Transform (Fig 9b), we find a characteristic frequency equal to 249 Hz, for the two modes. The characteristic spatial distance d_p is equal to 0.208 Do for mode 4 and 0.212 Do for mode 4. Then, Uc* is so equal to 0.34.
It shows that the two methods give the same order of Uc*.

6. Control of the radial fluctuations of the stagnation point.

6.1. Control of instabilities by modification of the central obstacle.

We used different geometries of obstacles: a disc, a cone and a spheroid. The last two obstacles have a length equal to the length of the zone of recirculation, which is 0,5Do. The profiles used are schematized on fig 6. For each form, measurements are taken for three values speed U_o= 8 m/s, 15 m/s and 30m/s (which corresponds to Reynolds numbers Re_{DO} calculated by using the external diameter Do: 28736, 53880 and 107760). For each speed, 1000 pairs of images of the jet are recorded. The results presented in this article are obtained for U_0 = 30 m/s.

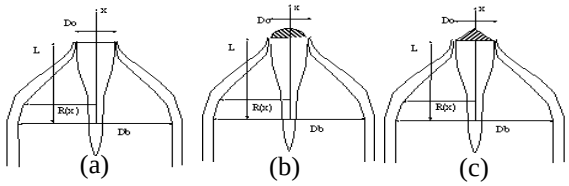

Fig 10: Profiles of the obstacles used for (a) basic annular jet, (b) spheroidal annular jet, (c) conical annular jet.

6.1.1 Basic annular jet

The results of PIV measurements were compared with the basic annular jet (Fig 11).

(a)

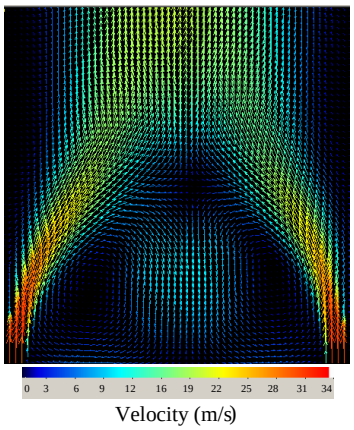

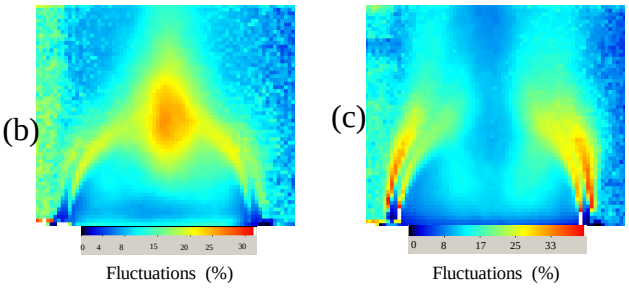

Fig 11: Basic annular jet: (a) average velocity field, (b) field of Reynolds decomposition radial velocities (c) field of Reynolds decomposition axial velocities.

6.1.2 Spheroidal annular jet

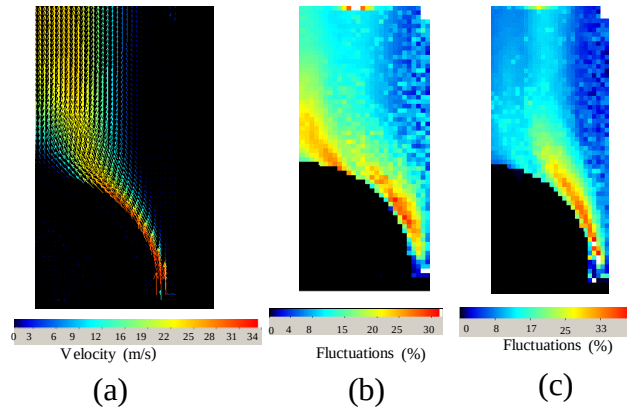

Fig 12: Spheroidal annular jet: (a) average velocity field, (b) field of Reynolds decomposition radial velocities (c) field of Reynolds decomposition axial velocities.

The average velocity field notes a complete disappearance of the zone of recirculation in the initial zone (Fig 12). The radial fluctuations are not any more on the level of the point of stagnation but rather on the level of the point of separation. A new zone of transverse fluctuations appears on the edges of the jet. These fluctuations are generated by the formation of the Kelvin-Helmholtz swirls in the external mixing layer. The axial fluctuations show that there is no more, in the case of a spheroidal obstacle, that only one zone of shearing. This result is a direct consequence of the disappearance of the recirculation zone. In fact, the air which is located downstream from the disc for the basic annular jet is replaced, for the spheroidal annular jet, by the obstacle.

6.1.3 Conical annular jet

The results are different when the obstacle used is a cone, as figure 13 shows it.

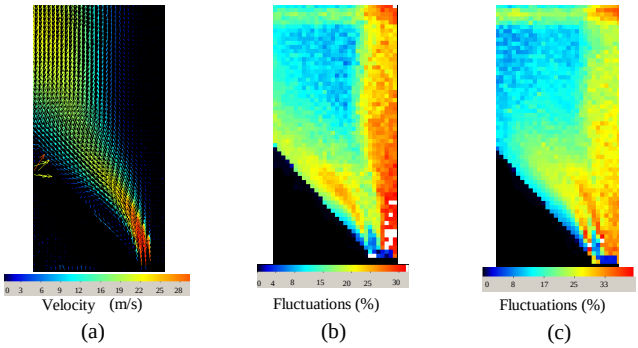

Fig 13: Conical annular jet: (a) average velocity field, (b) field of Reynolds decomposition radial velocities (c) field of Reynolds decomposition axial velocities.

The average velocity field shows a reduced recirculation zone at the exit of the jet. The radial fluctuations show that there are no more fluctuations on the level of the point of stagnation. This configuration seems to allow a passive control of this area of the jet. On the other hand, this annular jet also induced radial fluctuations on the edges of the jet. The obstacle does not allow the recirculation to become deformed towards the interior of the jet. This deformation thus occurs on outside and the radial fluctuations of the point of stagnation are transferred on the edge of the jet. The axial fluctuations show the presence of the two shear layers as in the case of the basic annular jet.

6.1.4 Comparison

Velocities profiles were plotted for different positions in the flow (Fig 8). The graph plotted in y=Do/4 (middle of the recirculation zone) underlines the preceding remarks: you can notice the presence of a recirculation zone (where speeds are negative) in the case of the basic and conical annular jets. For the spheroidal annular jet, the maximum speed is higher than for the two other configurations. Indeed, the spheroid occupies more space than the cone at the position that we study the velocities profile. By reducing open space for the development of the jet, this one would tend to be accelerated.

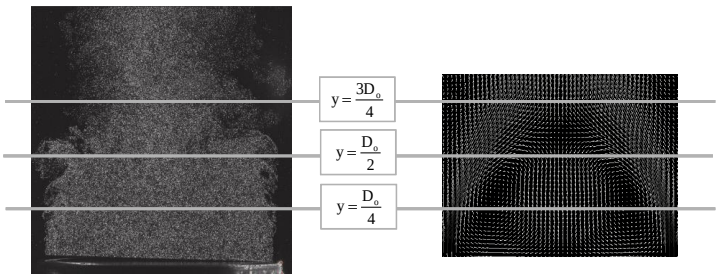

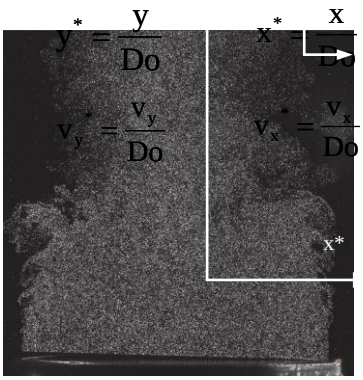

Fig 14: position of profiles and definitions

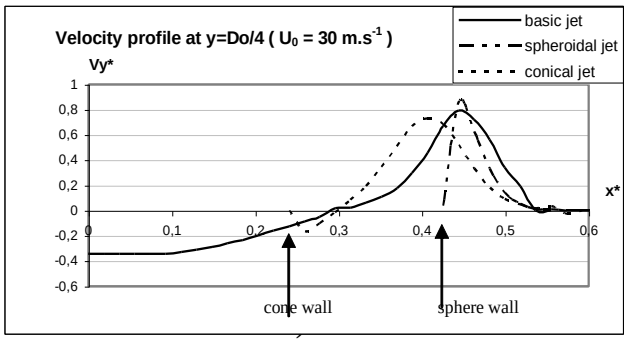

a)

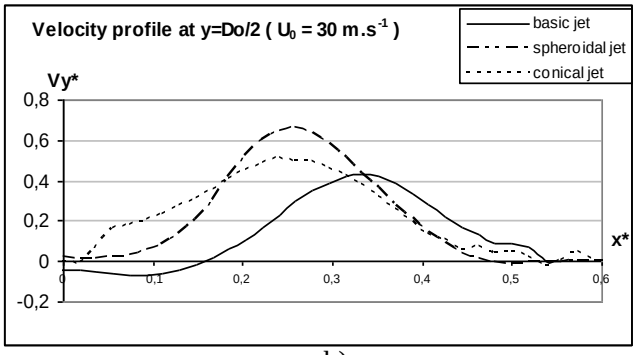

b)

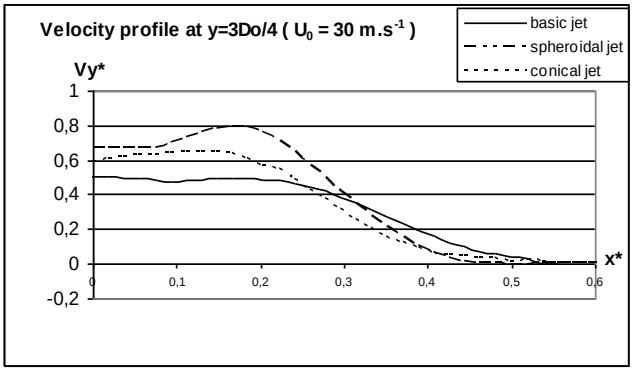

c)

Fig 15: Velocity profile a) y= Do/4, b) Do/2 c) 3Do/4 for basic jet, spheroidal jet and conical jet

In y=3Do/4 (in the intermediate zone, downstream from the point of stagnation), this same higher value for the spheroid is still found. It is noticeable that maximum speed extends from the center of the tube to x*=0.25 for the basic jet and x*=0.2 for the conical jet. This contracting of the zone of maximum speeds shows that the change of geometry of the central obstacle acts over the jet width. With the cone, this one thus tends to be tightened towards the central axis of the jet. This same phenomenon also occurs for the spheroidal jet. The spheroidal jet seems to generate a later recombination of the jet in the flow. The point of fastening, fixing the limit between the intermediate zone and the zone of fully developed jet must thus be further downstream than with the basic jet or the conical jet. The change of geometry of the central obstacle influences all the zones of the jet, and the whole of the characteristics of the flow.

6.2 Control by acoustic excitation

For industrial applications, a modification of the geometry of the jet is not easily possible. The second part of this study has the ambition to establish another control method of instabilities of an annular jet, by applying acoustic waves created by a loudspeaker place outside of the jet (the behaviour of the jet submitted to an acoustic excitation is independent of the loudspeaker position [16]).

The board of figure 16 shows the results obtained for a sweeping of 16 phases over one period of an acoustic wave of frequency 148Hz, with an amplitude of 3.62 V for the loudspeaker placed in front of the camera. This board enables us to see that the fields of an irregular way are different from one phase to another but from manner, rather irregular. It seems normal that the results are different according to the studied phase. If the acoustic wave comes at the good time on the stagnation point to then vibrate in an opposite way to this point the acoustic wave pushes back the jet so that the point of stagnation transversely remains motionless. On the other hand, if the wave comes on the stagnation point in a way, which actuates the jet with it, the wave accentuates the oscillation of the stagnation point which is then in resonance with the acoustic wave. The difference in phase between the beat of the jet and the

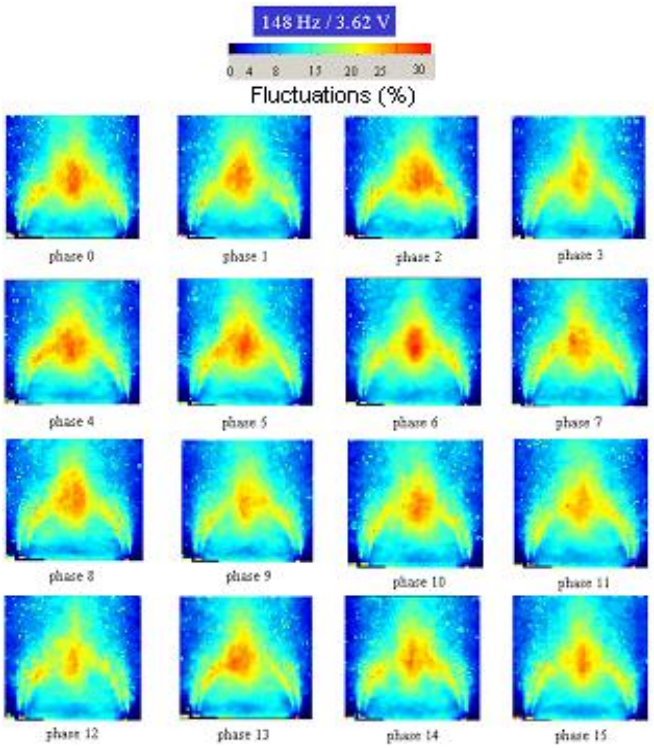

Fig 16: a sweeping of 16 phases over one period of an acoustic wave of frequency 148Hz, with amplitude of 3.62 V.

acoustic wave is thus a significant parameter to take into account to establish a control of the oscillations of the stagnation point. We can see that radial fluctuations of the stagnation point are much more significant for phase 2 than for phase 3.

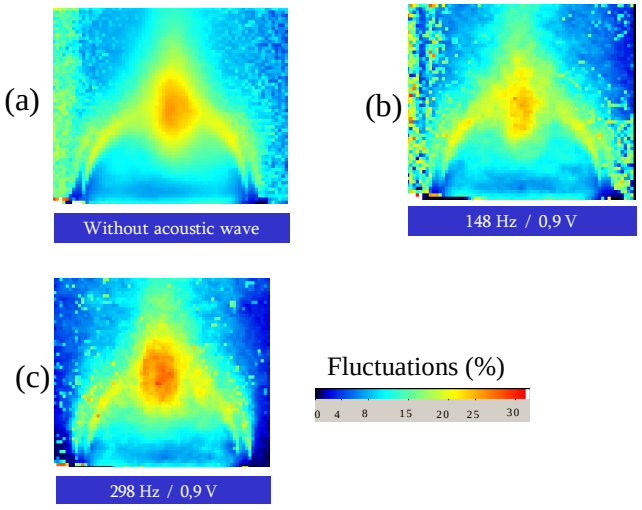

Fig 17: Field of Reynolds decomposition radial velocities: (a) without acoustics, (b) with acoustic excitations (f=148Hz), (c) with acoustic excitations (f=298Hz)

The fields of radial fluctuations calculated for the various phases with amplitude, frequency and position of the loudspeaker fixed, show significant differences: the radial fluctuations of the stagnation point are more or less strong according to the studied phase. The comparison of the radial fluctuations, for a given position of the loudspeaker, and different frequencies of excitation enables us to see that the radial fluctuations of the stagnation point are considerably reduced when the frequency of the acoustic wave is 148 Hz and are, on the other hand, larger for a frequency of 298 Hz. An example of these comparisons is illustrated on figure 17.

7 Conclusions

The study describes the recirculation zone of an annular jet by Particle Image Velocimetry. The Proper Orthogonal Decomposition has been applied to find the relationship of these radial fluctuations to the inner structures of the instantaneous P.I.V. fields. This statistical method can help to find the overall behaviour of the flow and to link fluctuations with typical modes. The P.O.D. analysis has shown that the flow could be decomposed into four main modes (90% of the total kinetic energy). Each one is responsible for a characteristic motion of the recirculation zone. The mode 0 represents the carrier flow, which is the most energetic. The space fluctuation of the stagnation point is principally due to the mode 1. Indeed, when the instantaneous fields are reconstructed with the modes without the first eigenfunction, the statistical analysis of these fields does not show local fluctuations. Measurements of convection velocities of primary vortices have been carried out, and a new method, from the temporal evolution of a P.O.D. mode applied on images has been used.

The modification of the geometry of the central obstacle is a possibility of passive control of the radial stagnation point fluctuations by using for example a conical annular jet. But this modification of the geometry of the jet is accompanied by new zones of fluctuations located on the edges of the jet. The study of active control by acoustic excitations is delicate with PIV measurements: it's necessary, in this case, to find a relation between the beat jet frequency, the frequency of the acoustic wave and the frequency of the images acquisition in order to know the real influence of the excitation on the flow. By putting the system of illumination and acquisition in phase with the acoustic wave, we can observe the response of a basic annular jet subjected to excitations of frequency equal to the natural frequency of stagnation point beat. These transversal oscillations are reduced for this frequency of excitation. A series of measurements coupling the techniques of P.I.V. and of hot wire Anemometry is considered by sweeping a frequency

band.

References:

[1] Chigier N.A. & Beer J.M., The flow region near the nozzle in double concentric jets, Journal of basics engineering, 1964.

[2]Ko N.W.M. & Chan W.T., Similarity in the initial region of annular jets: three configurations. J.Fluid Mech., 84, part 4, 1978, pp 641-656.

[3] Ko N.W.M. & Chan W.T., The inner regions of annular jets, J.Fluid Mech, 93, part 3, 1978, pp 549-584.

[4]Aly M.S and Rashed M.I.I. Experimental investigation of an annular jet. Journal of Wind Engineering and Industrial Aerodynamics, vol 37, 1991, pp 155-166.

[5] Adrian R.J., Christensen K.T. & Liu Z.C., Analysis and interpretation of instantaneous turbulent velocity fields, Experiment in Fluids, **29**, 2000, pp 275-290.

[6] Lumley J.L., Holmes P. & Berkooz G., The proper orthogonal decomposition in the analysis of turbulent flows, Annu. Rev. Fluid Mech, 25, 1993, pp 539-575.

[7]Lumley J.L., Holmes P. & Berkooz G., Turbulence, Coherent Structures, Dynamical Systems and Symmetry, Cambridge Monographs on Mechanics. Cambridge University Press. 1996.

[8]Moreau J., Patte-Rouland B., & Rouland E., Particle Image Velocimetry and Proper Orthogonal Decomposition., Euromech 411, – European Mechanics Society, section 5, 2000.

[9]Miozzi M. & Querzoli G., PTV and P.O.D. analysis of the instabilities in a quasi two-dimensionnel convective flow. Applied Scientific Research, 56, 1996, pp 221-242.

[10] Nakazano Y., Kiyomoto K., Uryu Y., Ohmori J., "Structures of an acoustically excited annular jet", Theoretical and applied mechanics, pp. 191-195 (1991).

[11] Travnicek Z., Tesar V, "Annular impinging jet with recirculation zone expanded by acoustic excitation", International Journal of Heat and Mass Transfer, vol 47, 2004, pp.2329-2341 (2004).

[12]Delville J., Characterisation of the Organisation in Shear Layers via the Proper Orthogonal Decomposition, Applied Scientific Research, 53, 1994, pp 263-281.

[13]Graftieux L., Michard M. & Grosjean N. Combining P.I.V., P.O.D. and vortex identification algorithms for the study of unsteady turbulent swirling flows. Euromech 411 – European Mechanics Society. 2000.

[14]Sirovish L., Method of snapshots, Quarterly of applied mathematical, 45(3), Brown University.
1987, pp 561-571,

[15]Patte-Rouland B., Lalizel G., Moreau J. and Rouland E. Flow analysis of an annular jet by Particle Image Velocimetry and Proper Orthogonal Decomposition. Measurement Science and Technology, 2001.

[16]Hwang S.D., Cho H.H. Effects of acoustic excitation positions on heat transfer and flow in axisymmetric impinging jet: main jet excitation and shear layer excitation. International Journal of Heat and Fluid Flow, 24, 2003, pp 199-209.